Polymerization transition in liquid AsS under pressure: An *ab initio* molecular dynamics study

Satoshi Ohmura and Fuyuki Shimojo

Department of Physics, Kumamoto University, Kumamoto 860-8555, Japan
(Received 17 October 2011; published 20 December 2011)

We study the pressure dependence of the structural and electronic properties of liquid AsS by *ab initio* molecular dynamics simulations. We confirm that liquid AsS consists of As_4S_4 molecules at ambient pressure, as in the crystalline state. With increasing pressure, a structural transition from molecular to polymeric liquid occurs near 2 GPa, which is eventually followed by metallization. The pressure dependence of the density and diffusion coefficients changes qualitatively with this transition. We find that, during metallization in the polymeric phase at higher pressures, the remnants of covalent interactions between atoms play an important role in the dynamics, i.e., the As-S bond length becomes longer with increasing pressure and the diffusion coefficients have a local maximum near 5 GPa. When the pressure approaches about 15 GPa, the covalent nature of the liquid becomes quite weak. These results explain recent experiments on the pressure dependence of the viscosity.

I. INTRODUCTION

The microscopic mechanism of structural changes in covalent materials under pressure is a topic of great interest in condensed-matter physics. From the geological viewpoint, not only well-known materials such as SiO_2, but arsenic chalcogenides, especially arsenic monosulfide AsS, which are formed at the boundary between the Earth's upper mantle and crust under pressures of 5–7 GPa, have also attracted considerable attention as minerals.[1] Under ambient conditions, crystalline realgar AsS has a monoclinic structure consisting of As_4S_4 molecules.[2,3] The molecule is made of As atoms threefold coordinated to two S and one As atoms with S atoms bridging two adjacent As atoms. At pressures of about 7 GPa, realgar AsS undergoes a polymorph transition to another molecular phase with a supposedly orthorhombic structure.[1]

It is known that, under low-pressure conditions, As_4S_4 molecules remain even upon melting. However, the structural properties and dynamics of liquid AsS under pressure are not well understood. Within the As_4S_4 molecule, atoms are connected by covalent bonds, so the rearrangement of the covalent bonds must occur under compression. While liquid arsenic chalcogenides show semiconducting properties at ambient conditions, high pressure leads to metallization. To investigate the microscopic mechanism of the pressure-induced semiconductor-metal (SC-M) transition, it is important to consider the relationship with the structural changes along with the rearrangement of the covalent bonds.

The temperature dependence of the SC-M transition in liquid arsenic chalcogenides has been extensively studied both experimentally[4–6] and theoretically.[7–10] The mechanism of this temperature-induced SC-M transition in liquid As_2S_3 and As_2Se_3 is closely related to the structural change with increasing temperature from the network to chainlike structure.[8–10] However, we are unaware of theoretical studies of the SC-M transition in liquid arsenic sulfides under pressure.

X-ray diffraction measurements of liquid AsS have clarified the pressure effects on structural properties,[11] and two structural changes have been proposed to occur with increasing pressure in the liquid state. The first structural change is from a molecular liquid to a nonmetallic polymerized liquid at 1.6–2.2 GPa. The second structural change is from this

nonmetallic polymerized liquid to a metallic liquid at 4.6–4.8 GPa. The viscosity of liquid AsS under high pressure has also been measured.[12] It is highly anomalous that the viscosity increases with pressure up to 2 GPa, after which it drops with further compression. For covalent liquids, the viscosity is strongly related to the covalent interactions, so studying the pressure effects on the bonding properties of liquid AsS to understand the pressure dependence of the viscosity is warranted.

In this paper, we investigate the structural and bonding properties and the dynamics of liquid AsS under pressure using *ab initio* molecular dynamics (MD) simulations. We have recently clarified the microscopic mechanisms of the pressure-induced SC-M transition in monatomic covalent liquid Se,[13] and this paper extends this research to compound covalent liquids. A key point to grasp in understanding the properties of this kind of liquid under pressure is that the covalent interactions remain in the metallic state, as indicated earlier for liquid Si (Refs. 14 and 15) as well as for liquid Se.[13] The purposes of our study are (1) to elucidate the microscopic relationship between the structural changes and the pressure-induced SC-M transition and (2) to clarify the pressure effects on the dynamic properties in relation to the covalent interactions in liquid AsS.

II. METHOD OF CALCULATION

In the MD simulations, a system of 160 (80As + 80S) atoms in a cubic supercell is used under periodic boundary conditions. The equations of motion for atoms are solved via an explicit reversible integrator[16] with a time step of $\Delta t = 2.0$ fs. A constant-pressure MD simulation[17] is performed for 4.8 ps at each given pressure to determine the density of the liquid state under pressure. Using the time-averaged density, the static and diffusion properties are investigated by MD simulations in the canonical ensemble[18,19] at a temperature of 1300 K. The quantities of interest are obtained by averaging over 14.4 ∼ 21.6 ps to achieve good statistics after the initial equilibration, which takes at least 2.4 ps.

The atomic forces are obtained from the electronic states calculated using the projector-augmented-wave method[20,21]
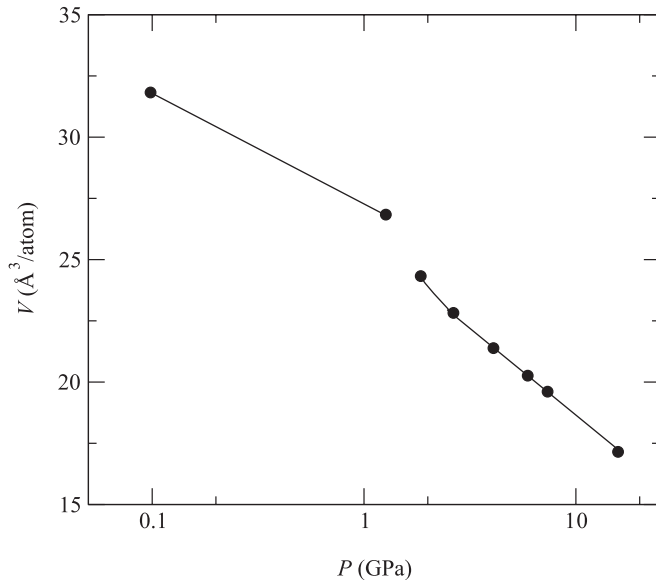
FIG. 1. Volume as a function of pressure for liquid AsS at 1300 K.

within the framework of density functional theory. Projector functions are generated for the $4s$, $4p$, and $4d$ states of As and the $3s$, $3p$, and $3d$ states of S. The plane-wave cutoff energies for the electronic pseudo-wave functions and the pseudo-charge density are 20 and 150 Ry, respectively. The exchange-correlation energy is treated by the generalized gradient approximation (GGA).[22] The Γ point is used for Brillouin zone sampling. The energy functional is minimized using an iterative scheme.[23,24]

III. RESULTS

A. Volume-pressure relation

The time-averaged pressure[25,26] is calculated at each density, and leads to the volume-pressure relation shown in Fig. 1. The thermodynamic states investigated in this study cover a density range from 2.79 to 5.17 g/cm³, and a pressure range from 0.1 to 15.8 GPa. Figure 1 shows that the pressure dependence of the volume changes qualitatively at around 2 GPa. This feature suggests that a first-order liquid-liquid transition occurs in liquid AsS, which is related to the transition from the molecular liquid to the polymeric liquid, as described in detail below.

B. Structure factor

Figure 2 shows the pressure dependence of the structure factor $S(k)$ of liquid AsS. The solid lines represent the calculated $S(k)$, which are obtained from the partial structure factors $S_{\alpha\beta}(k)$ with the x-ray scattering factors. The results of x-ray diffraction experiments[11] are indicated by open circles. The calculated results are in fairly good agreement with experiments. A remarkable feature exhibited in $S(k)$ is the first-sharp diffraction peak (FSDP) near $k = 1$ Å^{-1}. This peak reflects the existence of some structural characteristics in an intermediate range, such as the presence of As_4S_4 molecules below 2 GPa. The position of the FSDP gradually shifts to larger wave vectors and the intensity decreases with increasing
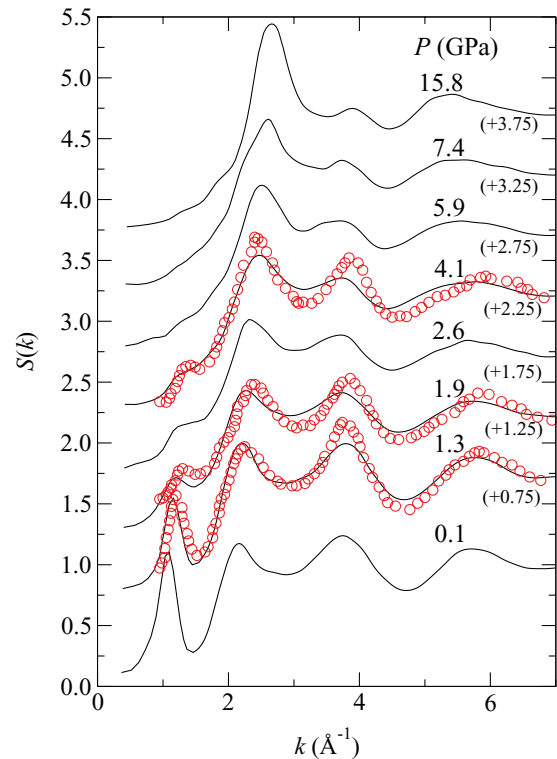
FIG. 2. (Color online) Pressure dependence of the total structure factor $S(k)$. The solid lines show the calculated $S(k)$, and the open circles represent the $S(k)$ obtained by x-ray diffraction measurements (Ref. 11). The curves are shifted vertically as indicated by the figures in parentheses.

pressure. Above 4.1 GPa, there is no clear FSDP. The height of the peak near $k = 2$ Å^{-1} increases with compression, whereas the peak height near $k = 4$ Å^{-1} decreases.

Figure 3 shows the pressure dependence of $S_{\alpha\beta}(k)$. We see that the FSDP shown in Fig. 2 is mainly determined by the As-As correlation, although the As-S correlation also contributes to forming the FSDP. The S-S correlation has only a shoulder at the position of FSDP. The intensities of these peaks decrease drastically for pressures above 1.3 GPa, which corresponds to the breakdown of As_4S_4 molecules in the liquid under compression. The peak of $S_{AsAs}(k)$ near $k = 2$ Å^{-1} splits into two peaks for pressures above 4.1 GPa. Above 2.6 GPa, a shoulder appears in $S_{SS}(k)$ near $k = 1.8$ Å^{-1}. The decrease of the intensity of the peak in $S(k)$ near $k = 4$ Å^{-1} originates from the decrease in the $S_{AsS}(k)$ peak.

C. Pair distribution function

The pressure dependence of the pair distribution functions $g_{\alpha\beta}(r)$ of liquid AsS is shown in Fig. 4. Since As_4S_4 molecules remain intact up to 1.3 GPa, the shape of $g_{\alpha\beta}(r)$ is almost unchanged. Above 1.9 GPa, $g_{\alpha\beta}(r)$ is largely different from those at lower pressures because the As_4S_4 molecule is broken. In particular, the first minimum and second peak of $g_{AsS}(r)$ disappear with increasing pressure. Note that, above 2.6 GPa, the peak reflecting to the formation of S-S homopolar bonds appears clearly near $r = 2.1$ Å in $g_{SS}(r)$. The S-S homopolar bond also exists in liquid As_2S_3 at ambient pressure.[27]
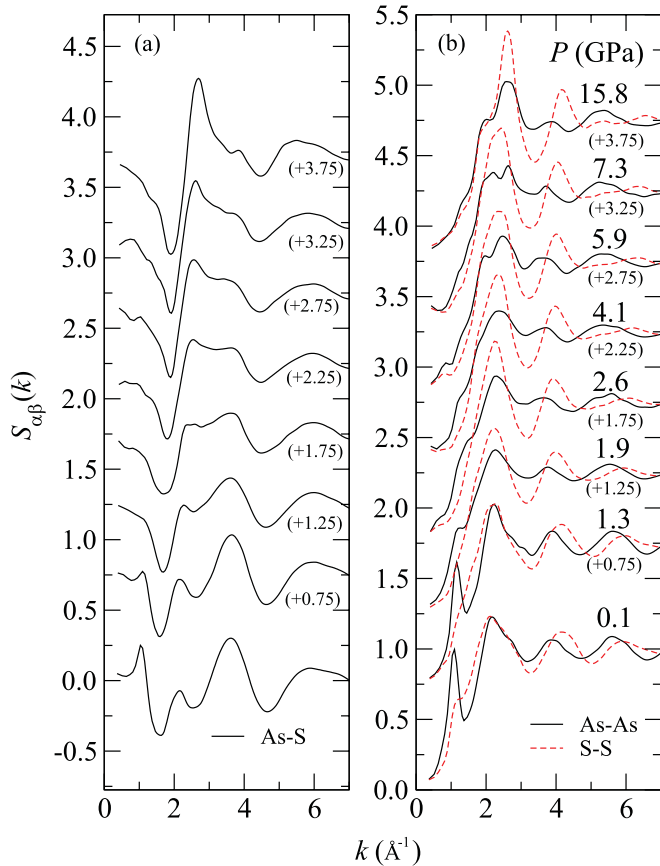
FIG. 3. (Color online) Pressure dependence of the partial structure factors $S_{\alpha\beta}(k)$. (a) The solid lines show $S_{AsS}(k)$. (b) The solid and dashed lines indicate $S_{AsAs}(k)$ and $S_{SS}(k)$, respectively. The curves are shifted vertically as indicated by the figures in parentheses.

Figure 5 shows the pressure dependence of the nearest-neighbor distances $r_{\alpha\beta}$ [the first-peak positions of $g_{\alpha\beta}(r)$]. In Fig. 5(c), the open circles indicate the position of the peak in $g_{SS}(r)$, which exists from ambient pressure, and the solid circles show the peak of the homopolar bonds above 2.6 GPa. At ambient pressure, r_{AsS}, r_{AsAs}, and r_{SS} are 2.62, 2.25, and 3.38 Å, respectively. These distances are almost the same as for the crystalline state[28] and remain almost unchanged up to 1.3 GPa. Above 1.9 GPa, the As-S and S-S covalent bonds lengthen gradually with increasing pressure, as indicated by the solid circles in Figs. 5(b) and 5(c), whereas no such change is seen in r_{AsAs} [Fig. 5(a)].

Figure 5(d) shows the pressure dependence of the partial coordination numbers $N_{\alpha\beta}$ for $\alpha\text{-}\beta = $ As-S (circles), As-As (squares), and S-S (diamonds). The coordination numbers are obtained in two ways: (I) $N_{\alpha\beta}^{(I)}$ are obtained by the integration of $4\pi r^2 \rho_\beta g_{\alpha\beta}(r)$ up to the first minimum position $r_{\alpha\beta}^{min}$ of $g_{\alpha\beta}(r)$ at 0.1 GPa for As-S and As-As, and at 2.6 GPa for S-S ($r_{AsS}^{min} = 2.7$, $r_{AsAs}^{min} = 3.0$, and $r_{SS}^{min} = 2.35$ Å), where ρ_β denotes the number density of β-type atoms. (II) $N_{\alpha\beta}^{(II)}$ are obtained by the integration of $4\pi r^2 \rho_\beta g_{\alpha\beta}(r)$ up to the first minimum of $r^2 g_{\alpha\beta}(r)$ at each pressure. At ambient pressure, $N_{AsS} = 2$ and $N_{AsAs} = 1$, irrespective of the method of calculation. These values are the same as for the crystalline state consisting of As$_4$S$_4$ molecules. Above 1.9 GPa, both N_{AsS}
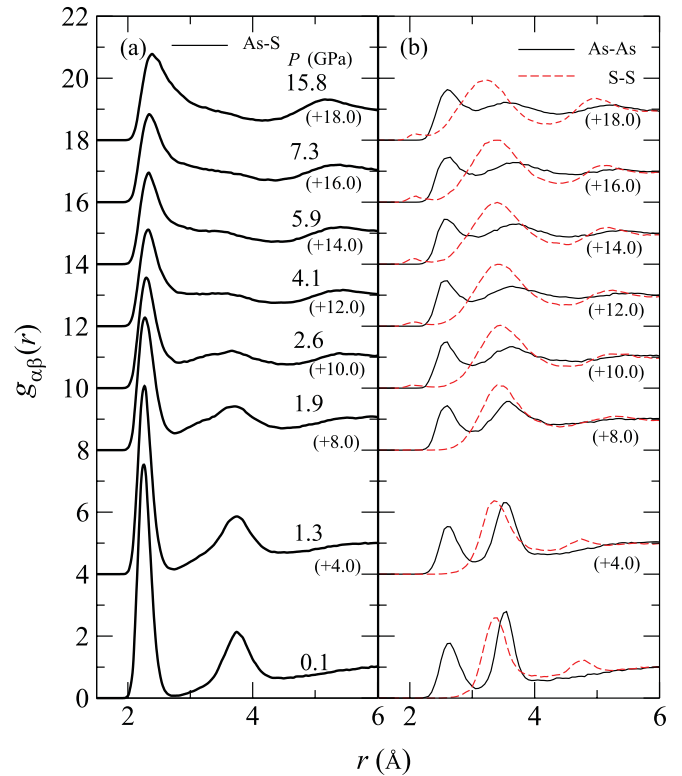
FIG. 4. (Color online) Pressure dependence of the pair distribution functions $g_{\alpha\beta}(r)$. (a) The solid lines show $g_{AsS}(r)$. (b) The solid and dashed lines indicate $g_{AsAs}(r)$ and $g_{SS}(r)$, respectively. The curves are shifted vertically as indicated by the figures in parentheses.

and N_{AsAs} begin to increase. Note that $N_{AsS}^{(II)}$ and $N_{AsAs}^{(II)}$ increase drastically above 10 GPa as shown by the solid symbols, which indicates that the first-coordination shell changes significantly in this pressure range, as discussed in Sec. IV. Above 2.6 GPa, N_{SS} has finite values, and increases with compression. Different from $N_{AsS}^{(II)}$ and $N_{AsAs}^{(II)}$, $N_{SS}^{(II)}$ does not show the sudden increase at pressures over 10 GPa, but keeps a similar value of about 0.1.

D. Electronic density of states

Figure 6 shows the pressure dependence of the total electronic density of states (DOS) $D(E)$ and the partial DOS $D_\alpha(E)$. The electronic states below -8 eV and above -6.5 eV originate mainly from the hybridization of s and p electrons, respectively. They are well separated from each other even for pressures up to 15.8 GPa. The DOS above E_F ($E = 0$) originates from p-like antibonding states. At 0.1 GPa, $D(E)$ has a small gap at E_F, which corresponds to the semiconducting properties of the liquid. Although the gap remains at pressures up to 1.3 GPa, the value of $D(E_F)$ becomes finite above 1.9 GPa, and increases with increasing pressure, which indicates that metallization follows the rupture of As$_4$S$_4$ molecules. It should, however, be noted that having a finite value of $D(E_F)$ does not directly prove that the system has the metallic properties. It is also well known that GGA underestimates band gaps in semiconductors. In addition to these facts, at pressures of 1.9–4.1 GPa, a deep dip is recognized at E_F. Therefore, we consider that the system
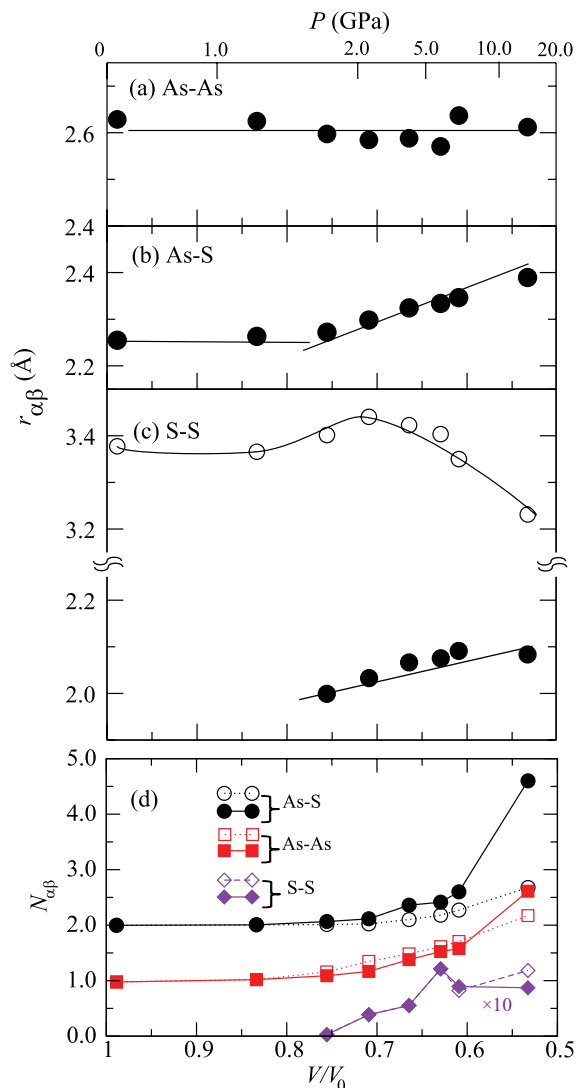
FIG. 5. (Color online) Pressure dependence of the nearest-neighbor distances $r_{\alpha\beta}$ for (a) α-β = As-As, (b) α-β = As-S, and (c) α-β = S-S. (d) Pressure dependence of the average coordination numbers $N_{\alpha\beta}$. The circles, squares, and diamonds show N_{AsS}, N_{AsAs} and N_{SS}, respectively. The open and solid symbols indicate $N_{\alpha\beta}^{(I)}$ and $N_{\alpha\beta}^{(II)}$, respectively (see text).

is not completely metallized but has some semiconducting properties over this pressure range even after polymerization. In this sense, our calculations are consistent with the experimental observations,[11] which suggest that nonmetallic polymerized liquid is metallized at 4.6–4.8 GPa. The shape of $D(E)$ does not change significantly for pressures above 4.1 GPa, indicating that metallization is completed at this pressure.

E. Bond-overlap population

We use population analysis[31,32] to clarify changes in bonding properties associated with compression. By expanding the electronic wave functions in an atomic-orbital basis set, we obtain the overlap population $O_{ij}(t)$ between the ith and jth atoms as a function of time t. $O_{ij}(t)$ gives a semiquantitative estimate of the strength of the covalentlike
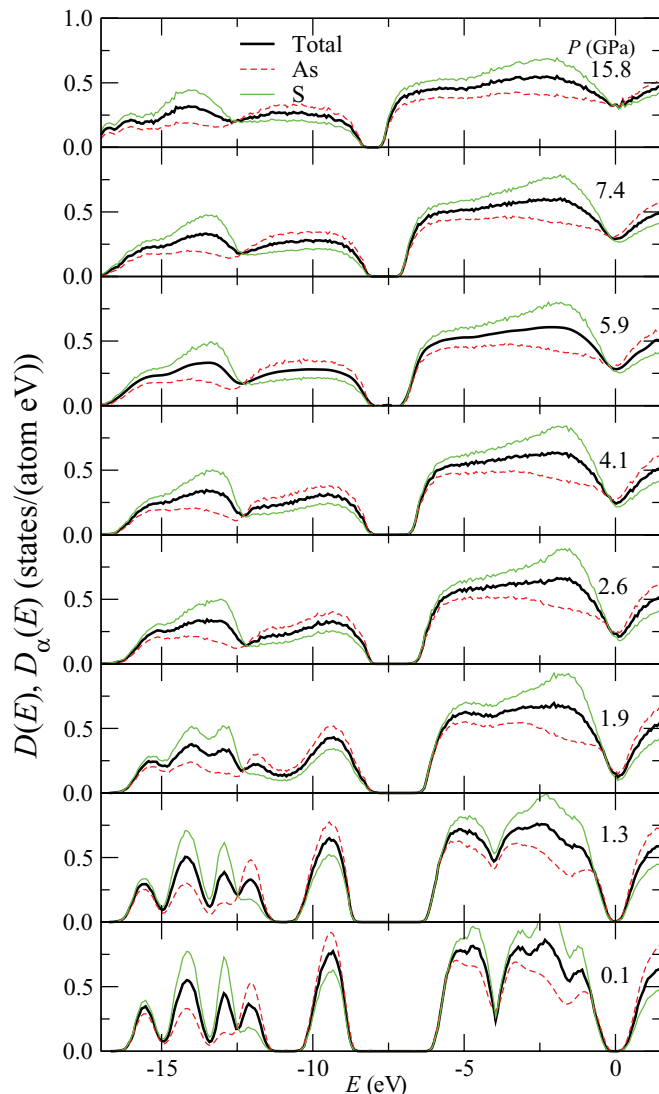
FIG. 6. (Color online) Pressure dependence of the electronic density of states $D(E)$ and the partial electronic density of states $D_{\alpha}(E)$. The bold-solid lines indicate $D(E)$. The thin-dashed and thin-solid lines show $D_{As}(E)$ and $D_S(E)$, respectively.

bonding between atoms. Note that $p_{\alpha\beta}(\overline{O})$ is normalized so that $\int_{O_{min}}^{\infty} p_{\alpha\beta}(\overline{O})\,d\overline{O}$ gives the average number of β-type atoms that have overlap populations greater than O_{min} around one α-type atom.

Figure 7 shows the time-averaged distribution $p_{\alpha\beta}(\overline{O})$ of the overlap populations $O_{ij}(t)$. In $p_{AsS}(\overline{O})$ and $p_{AsAs}(\overline{O})$, clear peaks exist near $\overline{O} = 0.7$ and $\overline{O} = 0.4$, respectively, up to 1.3 GPa, which reflects the covalent-bond interactions within As$_4$S$_4$ molecules. Above 1.3 GPa, $p_{AsS}(\overline{O})$ and $p_{AsAs}(\overline{O})$ increase with pressure in the ranges of $0 < \overline{O} < 0.5$ and $0 < \overline{O} < 0.3$, respectively, because bond exchange and bond rupture occur more frequently at higher pressures. Up to 5.9 GPa, the peaks in $p_{AsS}(\overline{O})$ and $p_{AsAs}(\overline{O})$ remain near $\overline{O} = 0.7$ and $\overline{O} = 0.4$, respectively, which indicates that the covalent interactions survive in this pressure range. The shift of these peaks to smaller $\overline{O}$ with increasing pressure means that the covalent interactions weaken, which is why r_{AsS} and
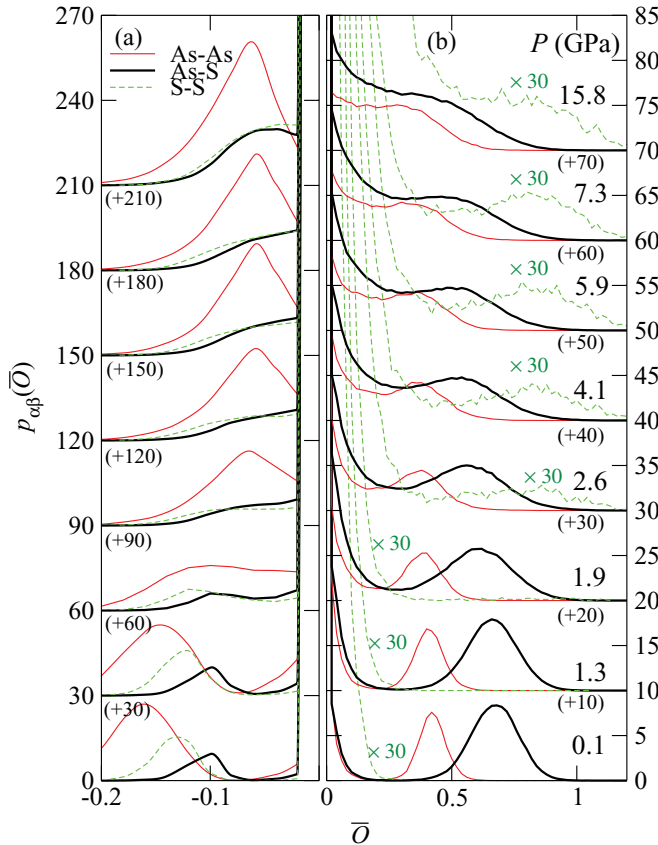
FIG. 7. (Color online) Pressure dependence of the distribution $p_{\alpha\beta}(\overline{O})$ of the bond-overlap populations for (a) $\overline{O} < 0$ and (b) $\overline{O} > 0$. The bold-solid, thin-solid, and thin-dashed lines indicate $p_{\mathrm{AsS}}(\overline{O})$, $p_{\mathrm{AsAs}}(\overline{O})$, and $p_{\mathrm{SS}}(\overline{O})$, respectively. In (b), $p_{\mathrm{SS}}(\overline{O})$ are enlarged to 30 times the original value. The curves are shifted vertically as indicated by the figures in parentheses.

r_{SS} increase with pressure, as indicated by the solid circles in Fig. 5. Above 2.6 GPa, $p_{\mathrm{SS}}(\overline{O})$ has a broad peak near $\overline{O} = 0.8$, which corresponds to the pressure-induced appearance of the S-S homopolar bonds. For $\overline{O} < 0$, the profiles of $p_{\alpha\beta}(\overline{O})$ are significantly different below and above 1.9 GPa, reflecting the transition from molecular to polymeric liquid.

F. Diffusion coefficient

The pressure dependence of the diffusion coefficients d_α is shown in Fig. 8. Up to 1.3 GPa, d_α decrease with increasing pressure, while keeping the As$_4$S$_4$ molecule intact. In molecular liquids, long-range molecular diffusion must occur in order for atoms to diffuse long range. As pressure increases from 0.1 to 1.3 GPa, the volume of the system largely decreases as shown in Fig. 1. Therefore, the free space between molecules is reduced and the molecular-diffusion path is significantly limited. In addition, we observed that direct interactions between molecules become stronger, i.e., new bonds are almost formed between neighboring molecules at 1.3 GPa. As a result, diffusion coefficients decrease rapidly.

Above 1.9 GPa, the pressure dependence changes qualitatively. Although the system exhibits metallic properties in the sense that there is no energy gap in the DOS at E_{F} in
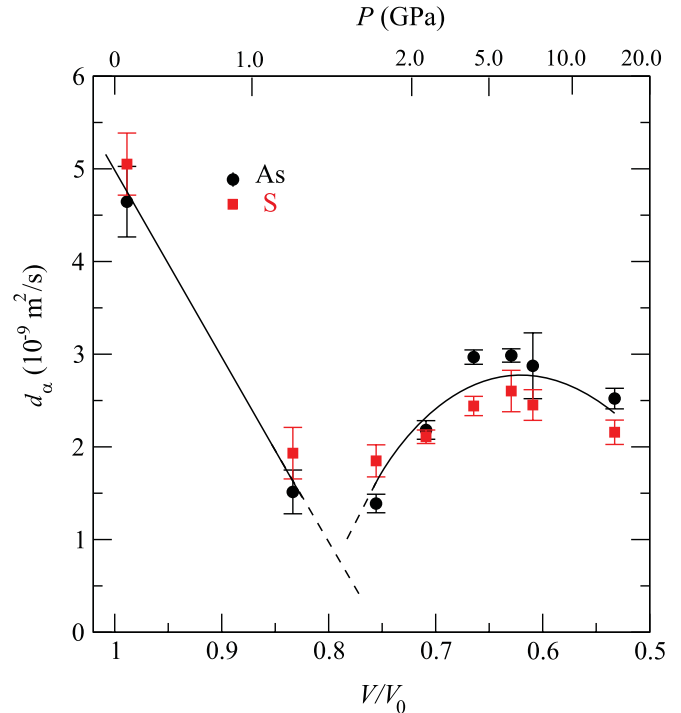
FIG. 8. (Color online) Pressure dependence of the diffusion coefficients d_α for $\alpha =$ As (circles) and $\alpha =$ S (squares).

this pressure range (as shown in Fig. 6), covalent interactions exist between atoms (as shown in Fig. 7). Since each bond weakens with an increase in the number of neighboring atoms, bond exchange occurs easily and frequently, and the diffusion coefficients increase above 1.9 GPa. Under further compression, d_α eventually decrease so that a local maximum occurs around 5 GPa, as seen in typical covalent liquids.[29,30] The pressure dependence of d_α corresponds well to the experimentally measured pressure dependence of the viscosity.[12] Note that the experimental measurements were performed just above the melting temperature at each pressure, whereas all simulations were carried out at 1300 K. However, changing the pressure in the order of GPa has a stronger effect than changing the temperature by an order of 100 K, as suggested by Fig. 2 of Ref. 12. Therefore, the qualitative pressure dependence of the calculated d_α agrees with that of the experimental viscosity. As for temperature dependence, the transition pressure of polymerization will increase and the diffusion maximum will appear more clearly when the temperature decreases.

IV. DISCUSSION

We discuss here the pressure-induced structural changes in relation to the covalent interactions. Each pair distribution function $g_{\alpha\beta}(r)$ is resolved according to the strength of the interatomic covalent bonds. The bold-dashed, thin-solid, and thin-dashed lines in Fig. 9 show $g_{\alpha\beta}^{(+)}(r)$, $g_{\alpha\beta}^{(-)}(r)$, and $g_{\alpha\beta}^{(0)}(r)$ obtained from atomic pairs with $O_{ij}(t) \geqslant \delta$, $O_{ij}(t) \leqslant -\delta$, and $-\delta < O_{ij}(t) < \delta$, respectively (we use $\delta = 0.01$). At 0.1 GPa, the first peak of $g_{\mathrm{AsS}}(r)$ consists of only $g_{\mathrm{AsS}}^{(+)}(r)$, whereas the second peak consists of mainly $g_{\mathrm{AsS}}^{(-)}(r)$. A similar profile
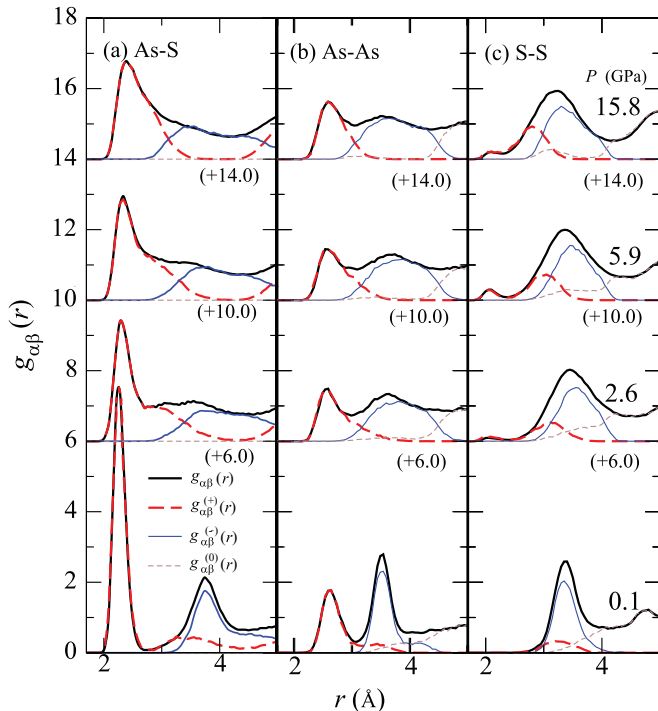
FIG. 9. (Color online) Pressure dependence of the pair distribution functions for (a) As-S, (b) As-As, and (c) S-S. The bold-dashed, thin-solid, and thin-dashed lines show $g_{\alpha\beta}^{(-)}(r)$ obtained for $O_{ij}(t) > \delta$, $g_{\alpha\beta}^{(+)}(r)$ for $O_{ij}(t) < -\delta$, and $g_{\alpha\beta}^{(0)}(r)$ for $-\delta < O_{ij}(t) < \delta$, respectively, with $\delta = 0.1$. The bold-solid lines indicate $g_{\alpha\beta}(r)$. The curves are shifted vertically as indicated by the figures in parentheses.

is apparent in $g_{\mathrm{AsAs}}(r)$, i.e., $g_{\mathrm{AsAs}}^{(+)}(r)$ and $g_{\mathrm{AsAs}}^{(-)}(r)$ form the first and second peaks, respectively, of $g_{\mathrm{AsAs}}(r)$. Note that $g_{\mathrm{AsS}}^{(+)}(r)$ and $g_{\mathrm{AsAs}}^{(+)}(r)$ have broad peaks at $3.2 \sim 3.5$ Å, which comes from intermolecular interactions, whereas the peaks of $g_{\mathrm{AsS}}^{(-)}(r)$ and $g_{\mathrm{AsAs}}^{(-)}(r)$ correspond to intramolecular interactions. With increasing pressure, the broad peaks of $g_{\mathrm{AsS}}^{(+)}(r)$ and $g_{\mathrm{AsAs}}^{(+)}(r)$ shift to smaller r, and merge into their respective first peaks. However, the peaks of $g_{\mathrm{AsS}}^{(-)}(r)$ and $g_{\mathrm{AsAs}}^{(-)}(r)$ remain well separated from their first peaks. These results mean that the increase in average coordination number accompanying the polymerization transition is due to bond formation between atoms belonging to different molecules; that is, after the transition, atoms belonging to different molecules come into the first coordination shell.

At 15.8 GPa, $g_{\mathrm{AsS}}^{(-)}(r)$ and $g_{\mathrm{AsAs}}^{(-)}(r)$ interpenetrate $g_{\mathrm{AsS}}^{(+)}(r)$ and $g_{\mathrm{AsAs}}^{(+)}(r)$, respectively. Consequently, the coordination numbers $N_{\mathrm{AsS}}^{(\mathrm{II})}$ and $N_{\mathrm{AsAs}}^{(\mathrm{II})}$ increase drastically, as shown in Fig. 5(d). We consider that the covalent nature of the liquid becomes quite weak in this pressure range.

Regarding the S-S correlation, $g_{\mathrm{SS}}^{(-)}(r)$, which originates from intramolecular correlation, provides the main contribution at 0.1 GPa to the peak of $g_{\mathrm{SS}}(r)$ at 3.3 Å. $g_{\mathrm{SS}}^{(+)}(r)$ also has a small peak, which corresponds to intermolecular interactions. These results show that no clear chemical bonds exist between S atoms at 0.1 GPa. With increasing pressure, a peak appears near 2.1 Å that consists of $g_{\mathrm{SS}}^{(+)}(r)$, which indicates the formation of S-S homopolar bonds between different molecules. Note that the peak of $g_{\mathrm{SS}}^{(+)}(r)$ near 3.3 Å shifts to smaller r with increasing pressure. At 15.8 GPa, this peak is almost at the same position as the peak of $g_{\mathrm{AsAs}}(r)$. This fact implies that the order in the atomic configuration, which originates from the covalent interactions that are a remnant of the molecular liquid, disappears at this pressure.

V. SUMMARY

By using *ab initio* molecular dynamics simulations, we have investigated the structural and bonding properties and the dynamics of liquid AsS under pressures up to 15.8 GPa. This work confirms that the metallization of liquid AsS follows the pressure-induced transition from molecular to polymeric liquid. The profiles of the bond-overlap populations show that covalent interactions persist in the metallic state, which determines the pressure dependence of the dynamic properties. After polymerization, the As-S bond lengthens with increasing pressure, and the diffusion coefficients exhibit a local maximum near 5 GPa.

[1]M. A. Tuktabiev, S. V. Popova, V. V. Brazhkin, A. G. Lyapin, and Y. Katayama, J. Phys.: Condens. Matter **21**, 385401 (2009).

[2]R. Zallen and M. L. Slade, Phys. Rev. B **18**, 5775 (1978).

[3]E. Hinze and J. Lauterjung, High Pressure Res. **4**, 324 (1990).

[4]K. Tamura, S. Hosokawa, M. Inui, M. Yao, H. Endo, and H. Hoshino, J. Non-Cryst. Solids **150**, 351 (1992).

[5]S. Hosokawa and K. Tamura, J. Phys.: Condens. Matter **16**, R1465 (2004).

[6]Y. Kajihara, M. Inui, K. Matsuda, K. Tamura, and S. Hosokawa, J. Non-Cryst. Solids **353**, 1985 (2007).

[7]X. F. Zhu and L. F. Chen, Phys. B (Amsterdam) **403**, 3302 (2008).

[8]F. Shimojo, S. Munejiri, K. Hoshino, and Y. Zempo, J. Phys.: Condens. Matter **11**, L153 (1999).

[9]F. Shimojo, S. Munejiri, K. Hoshino, and Y. Zempo, J. Phys.: Condens. Matter **12**, 6161 (2000).

[10]F. Shimojo, S. Munejiri, K. Hoshino, and Y. Zempo, J. Non-Cryst. Solids **312–314**, 349 (2002).

[11]V. V. Brazhkin, Y. Katayama, M. V. Kondrin, T. Hattori, A. G. Lyapin, and H. Saitoh, Phys. Rev. Lett. **100**, 145701 (2008).

[12]V. V. Brazhkin, M. Kanzaki, K. I. Funakoshi, and Y. Katayama, Phys. Rev. Lett. **102**, 115901 (2009).

[13]S. Ohmura and F. Shimojo, Phys. Rev. B **83**, 134206 (2011).

[14]I. Stich, M. Parrinello, and J. M. Holender, Phys. Rev. Lett. **76**, 2077 (1996).

[15]M. M. G. Alemany, M. Jain, L. Kronik, and J. R. Chelikowsky, Phys. Rev. B **69**, 075101 (2004).

[16]M. Tuckerman, B. J. Berne, and G. J. Martyna, J. Chem. Phys. **97**, 1990 (1992).

[17]G. J. Martyna, D. J. Tobias, and M. L. Klein, J. Chem. Phys. **101**, 4177 (1994).

[18]S. Nosé, Mol. Phys. **52**, 255 (1984).

[19]W. G. Hoover, Phys. Rev. A **31**, 1695 (1985).

[20]P. E. Blöchl, Phys. Rev. B **50**, 17953 (1994).

[21]G. Kresse and D. Joubert, Phys. Rev. B **59**, 1758 (1999).

[22]J. P. Perdew, K. Burke, and M. Ernzerhof, Phys. Rev. Lett. **77**, 3865 (1996).

[23]G. Kresse and J. Hafner, Phys. Rev. B **49**, 14251 (1994).

[24]F. Shimojo, R. K. Kalia, A. Nakano, and P. Vashishta, Comput. Phys. Commun. **140**, 303 (2001).

[25]O. H. Nielsen and R. M. Martin, Phys. Rev. B **32**, 3780 (1985).

[26]A. Dal Corso and R. Resta, Phys. Rev. B **50**, 4327 (1994).

[27]F. Shimojo, K. Hoshino, and Y. Zempo, J. Non-Cryst. Solids **312–314**, 388 (2002).

[28]P. Bonazzi, S. Menchetti, and G. Pratesi, Am. Mineral. **80**, 400 (1995).

[29]S. Ohmura and F. Shimojo, Phys. Rev. B **80**, 020202 (2009).

[30]S. Tsuneyuki and Y. Matsui, Phys. Rev. Lett. **74**, 3197 (1995).

[31]R. S. Mulliken, J. Chem. Phys. **23**, 1841 (1955).

[32]F. Shimojo, A. Nakano, R. K. Kalia, and P. Vashishta, Phys. Rev. E **77**, 066103 (2008).